Eur. Phys. J. D **7**, 573–576 (1999)

THE EUROPEAN PHYSICAL JOURNAL D

EDP Sciences

A computer simulation study of the ground-state configurations of Fe and Fe-Al clusters

O. Diéguez, R.C. Longo, C. Rey, and L.J. Gallego[a]

Departamento de Física de la Materia Condensada, Facultad de Física, Universidad de Santiago de Compostela, 15706 Santiago de Compostela, Spain

Received 29 April 1999

Abstract. Using the noncentral embedded atom model potential recently proposed by Besson and Morillo for $Fe_{1-y}Al_y$ bulk alloys ($y \leq 0.5$), we performed computer simulations to predict the ground-state configurations of Fe_n and $Fe_{n-x}Al_x$ clusters ($n \leq 19$). The computed structures of Fe_n clusters are in general agreement with such theoretical results as have been obtained by density functional calculations (*i.e.* for $n \leq 7$). The results for Fe-rich $Fe_{n-x}Al_x$ clusters show surface segregation of Al, which is in keeping with the findings of a previous study of $Ni_{n-x}Al_x$ clusters.

PACS. 36.40.-c Atomic and molecular clusters – 61.46.+w Clusters, nanoparticles, and nanocrystalline materials

1 Introduction

One of the fundamental problems of cluster research is the determination of the geometrical structures assumed by the clusters, which may affect their optical, magnetic and chemical properties, thermal stability and dynamical behaviour. Experimental information on cluster structures can be acquired by several means, including chemical probes [1,2] and the combination of photoionization and time-of-flight mass spectrometry [3]. However, in some cases cluster geometries cannot be determined with certainty by direct experimental methods, and theoretical studies provide an alternative means of gaining insight into the structural features of this kind of system.

Computation of the structures of clusters involving transition metal atoms by *ab initio* quantum mechanical methods is a very demanding computational task that is only feasible for very small clusters (see, *e.g.*, Refs. [4,5]). For this reason, most theoretical studies in this area have been based on semiempirical methods such as the embedded atom model (EAM) [6,7] and the tight-binding method (TBM) [8,9]. These studies have mainly focused on one-component clusters (see, *e.g.*, Ref. [10] and those cited therein), although some work on binary clusters has also been published. For instance, in reference [11] we reported the results of using molecular dynamics (MD) simulations based on the Voter and Chen (VC) version of the EAM [7] to compute the ground-state configurations of $Ni_{13-x}Al_x$, $Ni_{19-x}Al_x$ and $Ni_{55-x}Al_x$ clusters, and the same simulation technique has been used by Jellinek and Krissinel [12] to analyse the structures of $Ni_{13-x}Al_x$ clusters using a TBM potential [9].

The scarcity of EAM or TBM studies on binary clusters of metal atoms is probably largely due to the limited number of reliable model potentials for this kind of system. In this respect, a welcome contribution has recently been made by Besson and Morillo (BM) [13], who have developed an EAM noncentral potential for $Fe_{1-y}Al_y$ bulk alloys ($y \leq 0.5$). This potential has been extensively tested by evaluating its predictions for bulk and defect zero-temperature and temperature-dependent properties [13]. The aim of the work described here was to investigate its reliability for description of the structures of pure Fe_n and Fe-rich $Fe_{n-x}Al_x$ clusters with $n \leq 19$ (although its predictions for Al-rich clusters were also determined). The computed structures of the Fe_n clusters have been compared with theoretical predictions obtained by density functional calculations [4,5] or inferred from the results of chemical probe experiments [1], and those of the $Fe_{n-x}Al_x$ clusters with the results reported in reference [11] for $Ni_{n-x}Al_x$ clusters and with those of some theoretical studies of binary clusters of metal atoms [14–16].

In Section 2 we briefly describe the BM model potential and the computational procedure used in this paper to determine the ground-state cluster structures. In Section 3 we present and discuss the results, and finally, in Section 4, we summarize our main conclusions.

[a] e-mail: fmjavier@uscmail.usc.es

2 Summary of the model potential and the computational procedure

In the BM EAM potential [13], the energy of the Fe–Al system is given by

$$E = \sum_{i\in I_{\mathrm{Al}}} \left[F_{\mathrm{Al}}(\rho_i) + \frac{1}{2} \sum_{\substack{j\neq i \\ j\in I_{\mathrm{Al}}}} V_{\mathrm{AlAl}}(r_{ij}) + \alpha_{\mathrm{Al}} Y_i^2 \right] + \sum_{i\in I_{\mathrm{Fe}}} \left[F_{\mathrm{Fe}}(\rho_i) + \frac{1}{2} \sum_{\substack{j\neq i \\ j\in I_{\mathrm{Fe}}}} V_{\mathrm{FeFe}}(r_{ij}) + \alpha_{\mathrm{Fe}} Y_i^2 \right] + \sum_{\substack{i,j\neq i \\ i\in I_{\mathrm{Al}} \\ j\in I_{\mathrm{Fe}}}} V_{\mathrm{FeAl}}(r_{ij}) \quad (1)$$

where I_{Al} and I_{Fe} are the sets of indices of Al and Fe atoms, F_i and V_{ij} are respectively the embedding function and pair interaction, $\alpha_i Y_i^2$ is the noncentral interaction term, r_{ij} is the distance between atoms i and j, and ρ_i is the host electron density at site i, which is approximated by superimposing contributions by all the atoms surrounding atom i:

$$\rho_i = \sum_{j\neq i} f_j(r_{ij}) \quad (2)$$

$f_j(r_{ij})$ being the electron density of atom j at the position of the nucleus of atom i. Analytical expressions for the embedding functions, pair potentials, noncentral interactions and density functions are given in reference [13]. The parameters included in these expressions were optimized by Besson and Morillo [13] for prediction of the lattice constants, cohesive energies and elastic constants of pure Fe (*bcc*), pure Al (*fcc*) and the ordered compound FeAl (*B*2); it is these parameter values that have been used in the present study of Fe_n and $Fe_{n-x}Al_x$ clusters [17], in which ground-state structures were calculated by applying the steepest-descent method [18] to configurations generated along high-temperature MD trajectories, following a procedure similar to that employed in our study of $Ni_{n-x}Al_x$ clusters [11].

3 Results and discussion

Figure 1 shows the computed minimum energy structures and symmetries of pure Fe_n clusters ($3 \leq n \leq 19$). The predicted ground-state geometries of Fe_3 and Fe_4 (the equilateral triangle and the tetrahedron, respectively) agree with the results obtained by Chen *et al.* [4] using density functional theory. Density functional calculations for Fe_n clusters with $n \leq 7$ have also been performed by Ballone and Jones [5] using a simulated annealing approach based on the work of Car and Parrinello [19], and their results also agree, in general, with our BM EAM-based predictions for these clusters; the only slight discrepancy occurs for Fe_6, for which Ballone and Jones found the most stable structure to be a capped trigonal bipyramid that was, however, only 0.02 eV/atom more stable than the tetragonal bipyramid corresponding to the octahedral ground-state structure obtained in our calculations (Fig. 1). For Fe_n clusters with $n > 7$, no density functional results have as far as we know been published, but calculations recently performed by Andriotis and Menon [20] using a TB MD method predicted that Fe_{13} has an icosahedral structure, in keeping with our BM EAM predictions (Fig. 1). In should be pointed out that in spite of the good general agreement between our BM EAM results and density functional calculations for small Fe_n clusters, most of the Fe_n structures predicted by the latter method deviate somewhat from the symmetric structures predicted by the BM EAM potential [5].

Parks *et al.* [1] have studied the chemical reactivity of Fe_n clusters with small adsorbates such as H_2, D_2O and NH_3, and have interpreted their results in terms of structural differences between Fe_{14} and Fe_{15} and between Fe_{18} and Fe_{19}, suggesting likely geometries for Fe_{13}, Fe_{14}, Fe_{15} and Fe_{19}. In particular, the structures inferred as most probable for Fe_{13} and Fe_{19} are respectively the *fcc* cuboctahedron (or, alternatively, the *bcc* rhombic dodecahedron) and the *fcc* octahedron, although the icosahedral geometries obtained in our BM EAM calculations (Fig. 1) are not ruled out by the experimental findings. It should be borne in mind that the geometries revealed as most probable by chemical probe experiments are not necessarily those of the bare clusters, which can be altered by the adsorbates.

Figure 2 shows the calculated binding energies (the total minimum energies per atom, with the opposite sign) of all the Fe_n clusters studied in this paper. For comparison, in the same figure we also show the values reported by Chen *et al.* [4] for Fe_2, Fe_3 and Fe_4, and by Ballone and Jones [5] for $n \leq 7$. The binding energies computed in this work are much lower than those obtained by density functional calculations. This is doubtless because the parameters of the BM EAM potential were optimised using only bulk solid state properties (see Refs. [10,20]); had they been obtained using properties of the diatomic molecule as well as bulk solid properties, the computed binding energies of the clusters would no doubt be more accurate. It is nevertheless worth pointing out that the density functional results of Chen *et al.* and Ballone and Jones were obtained using the local spin density approximation, which tends to overestimate cluster binding energies (see, *e.g.*, Ref. [21]), so our binding energy results may be somewhat better than they appear to be in Figure 2.

Figure 3 shows the computed ground-state configurations of $Fe_{13-x}Al_x$ ($1 \leq x \leq 3$) and $Fe_{19-x}Al_x$ ($1 \leq x \leq 4$) clusters. All these Fe-rich binary clusters have the same basic icosahedral or double icosahedral structure as Fe_{13} and Fe_{19} respectively, and the Al atoms are located at the surface of the cluster in all cases. This latter result is in consonance with the common finding [14–16]

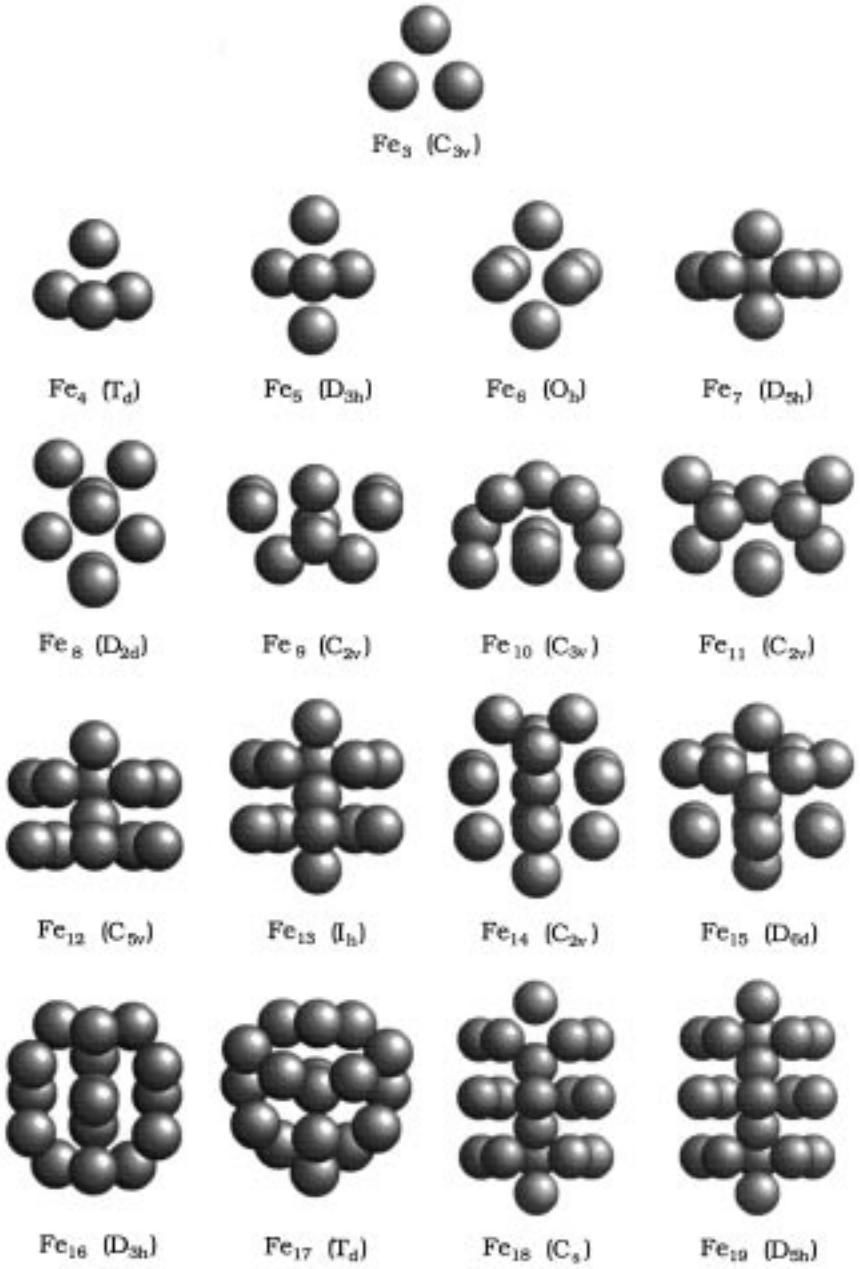

Fig. 1. Predicted minimum energy structures of Fe_n clusters ($3 \leq n \leq 19$), with their symmetries.

(corroborated by the results on Ni–Al clusters reported in Ref. [11]) that binary clusters of metal atoms exhibit surface segregation of the atom with the smaller surface energy (in this case Al [22]). By contrast, computed ground-state configurations of $Fe_{13-x}Al_x$ ($4 \leq x \leq 13$) and $Fe_{19-x}Al_x$ ($5 \leq x \leq 19$) are not icosahedral (results not shown). Since the BM EAM potential was developed for and tested on $Fe_{1-y}Al_y$ alloys with $y \leq 0.5$ [13], its application to $Fe_{n-x}Al_x$ clusters is expected to be less reliable for large x than small. At the high x extreme, computations performed by Yi *et al.* [23] using the Car-Parrinello method [19] predict that the most stable structures for Al_{13} and Al_{19} are the icosahedron and the octahedron respectively, results that are not reproduced by the BM EAM potential.

4 Summary and conclusions

In this work we performed MD simulations to compute the structures of Fe_n clusters ($n \leq 19$) and $Fe_{13-x}Al_x$ and $Fe_{19-x}Al_x$ clusters. The interactions between the atoms in the clusters were modelled using the n-body noncentral EAM potential developed by Besson and Morillo [13] for $Fe_{1-y}Al_y$ alloys ($y \leq 0.5$), the parameters of which were optimized for prediction of properties of pure Fe (*bcc*), pure Al (*fcc*) and the ordered FeAl phase ($B2$). The computed structures of Fe_n clusters were compared with results obtained from density functional calculations [4,5] and also with conclusions drawn from chemical reactivity experiments [1], although in this latter case comparison is not easy because the reactions used to probe the structure

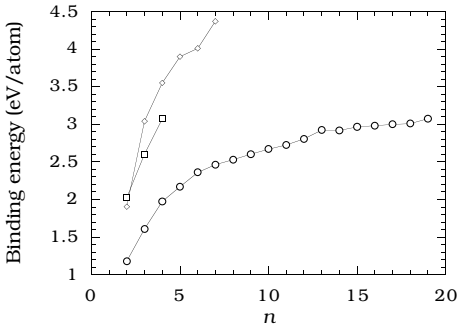

Fig. 2. Computed binding energies of Fe_n clusters (○). For comparison, the values obtained by Chen *et al.* [4] and Ballone and Jones [5] using density functional calculations are also shown (□ and ◇, respectively).

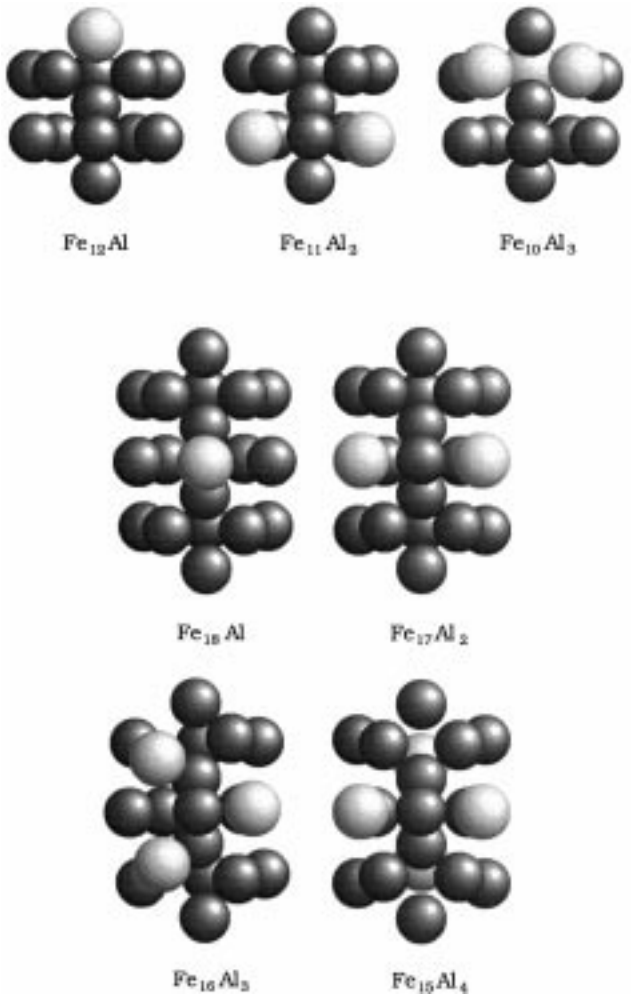

Fig. 3. Predicted minimum energy structures of $Fe_{13-x}Al_x$ ($1 \leq x \leq 3$) and $Fe_{19-x}Al_x$ ($1 \leq x \leq 4$) clusters.

of the clusters can induce structural changes. For small x, the computed structures of the $Fe_{n-x}Al_x$ clusters are in keeping with the results of previous studies of binary clusters of metal atoms [11,14–16]. In general, our results show that the BM EAM potential may be useful for qualitative description of the gross structural features of both pure Fe_n and Fe-rich $Fe_{n-x}Al_x$ clusters. The quality of the description is expected to be better for large n, *i.e.* in environments close to that used in the parameterization of the BM EAM potential; the BM EAM structures of the smaller Fe_n clusters fail to exhibit the asymmetries predicted, in most cases, by density functional calculations [5], and the BM EAM binding energies are much lower than those obtained by the latter methods. To improve description of the binding energies of Fe_n clusters we suggest that properties of the diatomic molecule be included among the data to which the BM EAM potential is fitted.

This work was supported by the DGICYT, Spain (Project No. PB95-0720-C02-02) and the Xunta de Galicia (Project Nos. XUGA20606B96 and PGIDT99PXI20604B).

References

1. E.K. Parks, B.H. Weiller, P.S. Bechthold, W.F. Hoffman, G.C. Nieman, L.G. Pobo, S.J. Riley, J. Chem. Phys. **88**, 1622 (1988).
2. E.K. Parks, B.J. Winter, T.D. Klots, S.J. Riley, J. Chem. Phys. **94**, 1882 (1991).
3. M. Pellarin, B. Baguenard, J.L. Vialle, J. Lermé, M. Broyer, J. Miller, A. Perez, Chem. Phys. Lett. **217**, 349 (1994).
4. J.L. Chen, C.S. Wang, K.A. Jackson, M.R. Pederson, Phys. Rev. B **44**, 6558 (1991).
5. P. Ballone, R.O. Jones, Chem. Phys. Lett. **233**, 632 (1995).
6. S.M. Foiles, M.I. Baskes, M.S. Daw, Phys. Rev. B **33**, 7983 (1986).
7. A.F. Voter, S.P. Chen, in *Characterization of Defects in Materials*, edited by R.W. Siegel, J.R. Weertman, R. Sinclair, MRS Symposia Proceedings No. 82 (Materials Research Society, Pittsburgh, 1987), p. 175.
8. F. Ducastelle, J. Phys. France **31**, 1055 (1970).
9. F. Cleri, V. Rosato, Phys. Rev. B **48**, 22 (1993).
10. C. Rey, L.J. Gallego, J. García-Rodeja, J.A. Alonso, M.P. Iñiguez, Phys. Rev. B **48**, 8253 (1993).
11. C. Rey, J. García-Rodeja, L.J. Gallego, Phys. Rev. B **54**, 2942 (1996).
12. J. Jellinek, E.B. Krissinel, Chem. Phys. Lett. **258**, 283 (1996).
13. R. Besson, J. Morillo, Phys. Rev. B **55**, 193 (1997).
14. L. Yang, T.J. Raeker, A.E. DePristo, Surf. Sci. **290**, 195 (1993).
15. J.M. Montejano-Carrizales, M.P. Iñiguez, J.A. Alonso, Phys. Rev. B **49**, 16649 (1994).
16. L. Zhu, A.E. DePristo, J. Chem. Phys. **102**, 5342 (1995).
17. We have detected two misprints in reference [13]: the value of the parameter ρ_0 for pure Fe shown in Table I should be 1.064×10^{-2}, rather than 9.80×10^{-3}, and the first minus sign on the right-hand side of equation (7b) should be a plus sign.
18. F.H. Stillinger, T.A. Weber, Phys. Rev. A **25**, 978 (1982).
19. R. Car, M. Parrinello, Phys. Rev. Lett. **55**, 2471 (1985).
20. A.N. Andriotis, M. Menon, Phys. Rev. B **57**, 10069 (1998).
21. P. Ballone, G. Galli, Phys. Rev. B **42**, 1112 (1990).
22. J.A. Alonso, N.H. March, *Electrons in Metals and Alloys* (Academic, New York, 1989).
23. J.-Y. Yi, D.J. Oh, J. Bernholc, R. Car, Chem. Phys. Lett. **174**, 461 (1990).